Korean J. Chem. Eng., 38(1), 204-214 (2021)
DOI: 10.1007/s11814-020-0679-y

pISSN: 0256-1115
eISSN: 1975-7220

Detrimental effect of industrial toluene organic impurities on the density of rigid polyurethane foam and their removal

Mohsen Mahmoudi and Jamshid Behin†

Advanced Chemical Engineering Research Center, Faculty of Petroleum and Chemical Engineering, Razi University, Kermanshah, Iran

(*Received 27 May 2020 • Revised 25 August 2020 • Accepted 18 September 2020*)

Abstract−The undesirable influence of organic impurities in toluene feedstock has been investigated on purity of synthesized Toluene diisocyanate and density of rigid polyurethane foam. Xylene, Ethyl cyclopentane, and Methyl benzothiophene were considered to represent three classes of impurities, including aromatics, non-aromatics, and sulfur-compounds, respectively. Statistical design of experiment using response surface methodology was applied for the quantification of the data acquired in pilot scale using impure Toluene model. Results showed that the concentration of 2-Nitro-4-isocyanatotoluene impurity in toluene diisocyanate and density of foam increased by 470% and 42%, respectively, for the examined rate of toluene impurity. Moreover, SEM graphs revealed that cell size and number of closed-cells decreased by ~55%, producing more open cells. Ethyl cyclopentane had the most effect (74.4%) on density among the variables investigated. Subsequently, an activated carbon-based adsorptive process was implemented in laboratory batch mode at 20±1 °C to achieve an appropriate level of impurity in industrial-grade toluene. The simultaneous-competitive adsorption of three classes of described impurities was carried out and the highest adsorption capacity of 7.3, 47.4, and 161.5 mg/g was achieved for aromatics, non-aromatics, and sulfur compounds, respectively. The Langmuir isotherm model exhibits satisfactory equilibrium data for non-aromatics and sulfur compounds and for aromatics the Freundlich was the best one.

Keywords: Polyurethane Foam Defect, Toluene Organic Impurities, 2-Nitro-4-isocyanatotoluene, Competitive Adsorption, Foam Density, Non-aromatics

INTRODUCTION

Rigid polyurethane foam (PUF) is one of the most valuable commercial foams with a high compression resistance to mass ratio [1-3]. Because of high thermal resistivity and low density, it was used industrially to insulate ships, LNG cargos, refrigerators, containers, tanks, and pipes. One of the key factors regulating morphological, mechanical, and thermal properties of PUF is apparent density [4,5]. PU monomer is synthesized from a mixture of polyol and isocyanate where an exothermic reaction is happening between the functional groups of isocyanate (-N=C=O) and hydroxyl [6,7],

$$n(R_{iso}-NCO)+n(R_{polyol}-OH)\rightarrow n(R_{iso}-NH-COO-R_{polyol})\rightarrow(-R_{iso}-NH-COO-R_{polyol}-)_n \quad (1)$$

where R_{iso} and R_{polyol} were derived from the isocyanate and polyol monomer, respectively.

Its spongy property is associated with the simultaneous hybridization of aforementioned polymerization reaction and isocyanate-water (most widely used blowing agent) expansion reaction as follows [8,9]:

$$2(R_{iso}-NCO)+H_2O\rightarrow R_{iso}-NH-CO-HN-R_{iso}+CO_2 \quad (2)$$

The type and quantity of the isocyanate used are the key factors in that way more isocyanate mass ratio leads to more hard segments and more rigid PUF [10]. Toluene diisocyanate (TDI) is the most commonly form for the synthesis rigid PUF of high glass transition and tensile strength [11-13]. 2,4- and 2,6-TDI isomers (mass ratio: 80/20) are industrially produced by nitration of toluene in sulfuric acid medium to dinitrotoluene (DNT), then by catalytic reduction to toluenediamine followed by conversion of amino groups to isocyanates via phosgenation reaction [14].

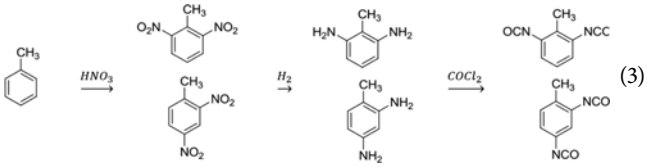

(3)

Several studies were conducted to establish the influence of density on rigid PUF characteristics. Density variability was shown to be associated with the cell size and cell-wall thickness affecting water absorption and thermal conductivity [15-17]. The TDI impurity is a key factor affecting the PUF density. Toluene, as a raw material for TDI production, is obtained by catalytic naphtha reformation followed by fractionation operations. In its industrial grade, some kinds of undesirable impurities (C_7-C_9 cyclic hydrocarbons) can occur such as aromatic compounds (mainly xylene), non-aromatics compounds (mainly ethyl cyclopentane), and sulfur compounds (mainly methyl benzothiophene) [18]. The adsorption of these impurities on palladium chloride hampers the normal function of hydrogenation catalyst and leads to a decrease in DNT to toluenediamine conversion [19]. The reaction of unreacted DNT in phosgenation reactor results

†To whom correspondence should be addressed.
E-mail: Behin@razi.ac.ir

in formation of 2-Nitro-4-isocyanatotoluene ($C_8H_6N_2O_3$) as a main impurity of TDI in commercial plant. The formation of other minor impurity such as alkyl hydrogen sulphates ($-CH_2OSO_3H$) is also observed due to toluene impurities.

Karoon Petrochemical Company is a pioneer in TDI production in Iran and even in the Middle East. The toluene feed often contains three classes of impurities: aromatics of maximum 100 ppm, non-aromatics of maximum 200 ppm, and sulfur compounds of maximum 300 ppm under the worst conditions. However, a non-aromatics content of maximum 200 ppm is unavoidable as a single impurity under normal conditions. In addition, the research on the sorption of coexisting aromatic, non-aromatic, and sulfur impurities from organic solvents is very scarce and has not yet been investigated to the best of the knowledge of the authors.

Therefore, the effects of the aforementioned impurities on the concentration of 2-Nitro-4-isocyanatotoluene (NIC) in TDI and subsequent PUF density were examined in the first part of the experiments. For this reason, a model mixture of three impurities in pure toluene was prepared and fed in pilot plant. Response surface methodology based on central composite design (RSM-CCD) was applied to reduce the use of chemicals and the number of test runs. The goal of the second part of experiments was to study the kinetic and thermodynamic of impurities adsorption from toluene as an organic phase with activated carbon (AC).

EXPERIMENTAL

1. Materials

All reagents including Xylene (purity ≥98.5%), ethylcyclopentane (purity 97%), methyl benzothiophene (purity 96%), Nitric acid (purity >90%), sulfuric acid (purity 95.5-96.5 %), palladium (II) chloride (purity 99%), 1,4-Butanediol (purity 99%), and N,N,N′,N″,N″ pentamethyl diethylene triamine (PMDETA) of purity 99% were obtained from Sigma Aldrich, Germany. Polyol (Daltolac R 180, Sucrose-based polyether polyol) of following characteristic was obtained from Huntsman co., Thailand (hydroxyl value: 440 mgKOH/g, functionality: 4.3, specific gravity: 1.1 and viscosity 5,500 cP at 25 °C).

Table 1. Levels of impurities concentration (mg/L)

Factors	Symbol	Actual and coded level				
		−2	−1	0	+1	+2
Xylene	X_1	37	48	64	80	91
Ethyl cyclopentane	X_2	19	50	95	140	170
Methyl benzothiophene	X_3	35	85	157	230	280

2. Pilot Plant

The first part of the experiments focused on investigating the effect of toluene feed impurities as independent variables (X_i) on the concentration of NIC in TDI (Y_1) and the quality of PUF by measuring density as the response variable (Y_2). The impure form of toluene was made with xylene, ethyl cyclopentane, and methyl benzothiophene. Table 1 illustrates the coded and actual levels of variables. The levels of variables were chosen according to the lowest (good) and the highest (worst) impurity content of industrial grade toluene feed.

Impure toluene feed was converted to TDI in pilot plant comprising units of nitration (Fig. 1(a)), hydrogenation (Fig. 1(b)), and

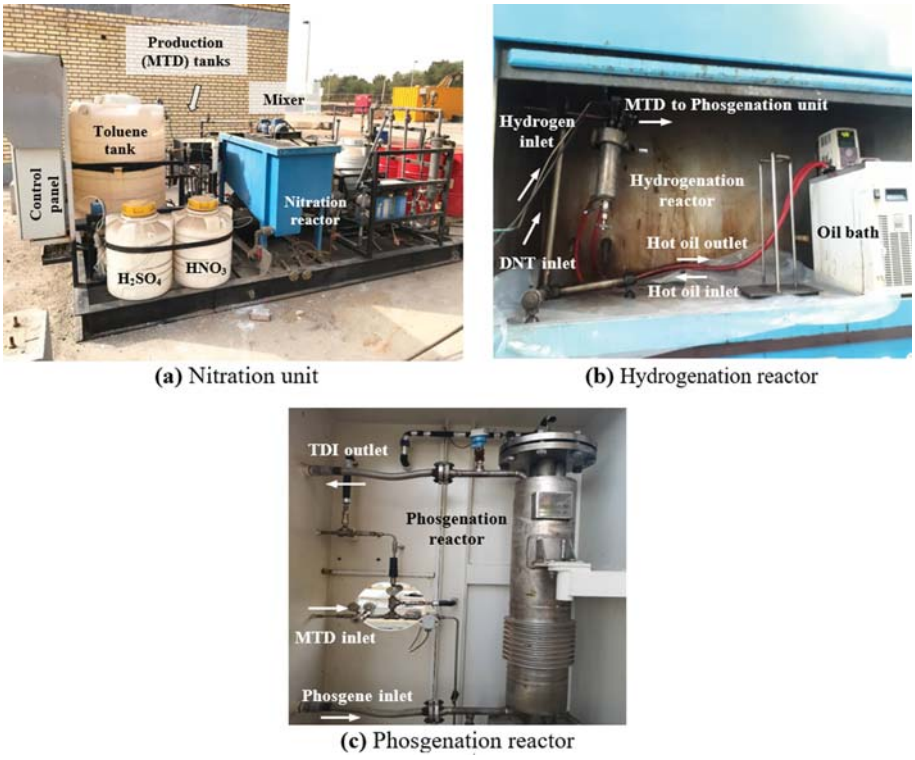

(a) Nitration unit (b) Hydrogenation reactor

(c) Phosgenation reactor

Fig. 1. Pilot plant of TDI production.

phosgenation (Fig. 1(c)), all owned by Karoon Petrochemical Co., Iran. Toluene and concentrated nitric acid (64%) were mixed in the nitration reactor (capacity: 210 L, perfluoroalkoxy alkane) equipped with a mixer at room temperature. Concentrated sulfuric acid was then gradually added to the mixture in 15 min. The mixture was washed with distilled water after 15 min of reaction, in order to obtain DNT. The hydrogenation reactor (capacity: 1 L, stainless steel) was filled with the palladium (II) chloride (catalyst) slurry and DNT solution before the hydrogenation process was started. Hydrogen gas was supplied from a high-pressure cylinder, passed via a mass flow controller and introduced into the hydrogenation reactor at 3 bar and 120 °C equipped with hot oil circulation system. After the purification steps (not discussed), the formed MTD and phosgene reacted at 160 °C in benzene as an inert solvent within 26 L reactor (inconel) to form intermediate carbamoyl chloride. Afterwards, the reaction temperature was increased to ~175 °C to form TDI from the intermediate product. Eventually, distillation and evaporation processes purified the synthesized TDI and finally it was sent to the storage vessel for further use. However, among the other impurities, the NIC remained in the product that was not separated by conventional distillation. The concentration of NIC in TDI was measured by gas chromatography GC/MSeMS (Agilent 7,890B MSD 7,000C, Germany) and the NCO content of TDI samples was determined according to the Chinese standard HG-T2409-1992 [20].

3. Foam Preparation

PUF samples were prepared from TDI in batch scale. They were synthesized by one-step and free-rising method, which the reactants (according to Table 2) were poured into an open mold to produce free-rise foam. Required quantities of polyol, catalysts, 1,4-Butanediol, and distilled water (blowing agent) were mixed using a mechanical stirrer at 2,200 rpm for 60 s. Then, TDI was easily added to the mixture and stirred at the same rotation speed for about 7-10 s. The mixture had been poured into a mold and allowed the foam to rise and sit for one day at ambient temperature. The apparent density of the sample with the size of 30×30×30 mm was determined according to ASTM D1622 method [21]. In each run, five measurements were performed and the mean value was reported. An air pycnometer measured the closed cell content of 20 mm cubic foam in size according to ASTM D2850-15 [22]. The chemical composition of PUF involving polyol, catalyst, and blowing agent was kept constant in all samples except for TDI impurity. Moreover, as density is the main variable controlling most of the mechanical properties of foam, the others such as hardness, tensile strength, elongation, compression set, resilience, tear strength, and shrinkage were not tested in this work.

4. Multicomponent Adsorption

In the second part of experimental studies, an industrial-grade Toluene with the highest initial concentration of impurities (worst practical conditions) was subjected to a batch-mode adsorption cycle on AC. All impurities were classified into three key groups, including aromatics, non-aromatics, and sulfur compounds, as there is not enough knowledge about the exact chemical compositions of each category in toluene feedstock. Moreover, the GC method of analysis is able to identify only the class of impurities in real feed. Therefore, 500 mL of impure toluene was poured in the jacketed Pyrex chamber at a desired constant temperature at each experimental phase. Then, one-gram AC was added to liquid. The solution was stirred continuously at a constant stirring rate (500 rpm) and under temperature-controlled system (Aqualytic, Germany). A liquid sample (5 mL) was taken for further analysis after every 3 h (assuming reaching equilibrium condition upon the preliminary experiments) and another one-gram AC was added to the suspension for the next 3 h. This procedure was followed until a cumulative period of 15 h in which 5 g AC was added to the mixture. The collected liquid sample was filtered and subjected to analysis. The initial and final concentration of the impurities was measured by gas chromatography. Diahope AC (Mitsubishi Kasei, Japan) with microporous structure (pore volume: 0.7 mL/g, average pore diameter. 1.2 nm and BET surface area: 1,150 m^2/g) was employed in the adsorption process. The adsorption capacity was determined from the following equation:

$$q_e = \frac{(C_o - C_e)\cdot V}{m} \tag{4}$$

where m (g), V (L), C_o and C_e (mg/L) are mass of adsorbent (AC), volume of solution, and initial and equilibrium concentrations of impurities, respectively.

To evaluate the rate of the non-aromatics adsorption on solid surface, two kinetic models were used. The pseudo-first-order model is described as:

$$\text{Ln}\,(q_e - q_t) = \text{Ln}\,q_e - k_1\cdot t \tag{5}$$

and the pseudo-second-order model:

$$\frac{t}{q_t} = \frac{1}{k_2 q_e^2} + \frac{t}{q_e} \tag{6}$$

where k_1 (1/min) and k_2 (g/mg min) are the constants of adsorption rate.

Moreover, two sorption isotherms were examined involving nonlinear form of Langmuir model (Eq. (7)), assuming that adsorption can only occur at a finite number of different sites with monolayer thickness, and Freundlich model (Eq. (8)) characterizing the nonideal and reversible multilayer adsorption.

$$q_e = \frac{q_m K_L C_e}{1 + K_L C_e} \tag{7}$$

Table 2. Chemical compositions of rigid polyurethane foam (PUF)

Precursor	Polyol	PMDETA	Distilled water	1,4-Butanediol†	TDI
phr*	100	0.5	2.65	100	115

*Represents as parts per hundred of polyols by weight

†Chain extender

$$q_e = K_F C_e^{1/n} \quad (8)$$

where K_L (L/mg), q_e (mg/g) and q_m (mg/g) represent, respectively, the energy/net enthalpy of the adsorption, the equilibrium, and maximum adsorption capacity, and "n" and K_F (L^n $mg^{1/n}$/g) are the Freundlich constants representing favorability and capacity of adsorption, respectively.

The change in Gibbs free energy of the adsorption phenomenon is defined by the following relation:

$$\Delta G^o = -RT \ln K_{eq} \quad (9)$$

where K_{eq} (q_e/C_e) is the equilibrium constant.

The differences in thermodynamic parameters, i.e., standard entropy (ΔS^o) and enthalpy (ΔH^o) indicating the spontaneity and heat change of the adsorption phenomenon, can be determined from the intercept and slope of the van't Hoff equation, respectively.

$$\ln K_{eq} = \frac{\Delta S^o}{R} - \frac{\Delta H^o}{R}\left(\frac{1}{T}\right) \quad (10)$$

RESULTS AND DISCUSSION

1. Effect of Toluene Impurities on TDI and PUF

RSM with CCD was applied with six replications at central point

Table 3. Design of experiment along with independent and response variables

Run no.	Independent variables, X_i			Response variables, Y_i			
	Concentration of impurities (mg/L)			Concentration of NIC (mg/L)		Density of PUF (kg/m^3)	
	Xylene	Ethyl cyclopentane	Methyl benzothiophene	Actual	Predicted	Actual	Predicted
1	−1	−1	−1	19.2	17.054	26.920	27.378
2	1	−1	−1	29.0	28.079	28.104	28.460
3	−1	1	−1	61.8	61.954	33.490	33.408
4	1	1	−1	71.5	72.979	34.674	34.490
5	−1	−1	1	41.7	41.129	30.545	30.686
6	1	−1	1	46.5	52.154	31.729	31.768
7	−1	1	1	89.1	86.029	37.115	36.716
8	1	1	1	109.4	97.054	38.299	37.798
9	−2	0	0	45.2	43.207	31.598	31.506
10	2	0	0	67.0	65.257	33.559	33.670
11	0	−2	0	23.1	20.621	27.049	26.558
12	0	2	0	105	110.421	38.028	38.618
13	0	0	−2	35.6	30.157	29.547	29.280
14	0	0	2	79.3	78.307	35.528	35.896
15	0	0	0	51.3	54.232	32.590	32.588
16	0	0	0	52.1	54.232	32.597	32.588
17	0	0	0	49.0	54.232	32.586	32.588
18	0	0	0	55.7	54.232	32.604	32.588
19	0	0	0	50.0	54.232	32.600	32.588
20	0	0	0	48.3	54.232	32.595	32.588

Table 4. Analysis of variance for the response functions

Source	DF		Adj SS		Adj MS		F-value		p-Value	
	Y_1	Y_2	Y_1	Y_2	Y_1	Y_2	Y_1	Y_2	Y_1	Y_2
Model	4	3	11,085.3	193.881	2,771.32	64.627	112.13	635.98	<0.0001	<0.0001
Linear	3	3	10,868.7	193.881	3,622.89	64.627	146.58	635.98	<0.0001	<0.0001
X_1	1	1	486.2	4.685	486.20	4.685	19.67	46.10	0.002	<0.0001
X_2	1	1	8,064.0	145.432	8,064.04	145.432	326.28	1,431.15	<0.0001	<0.0001
X_3	1	1	2,318.4	43.765	2,318.42	43.765	93.80	430.68	<0.0001	<0.0001
X_2^2	1		216.6		216.62		8.76		0.01	
Error	15	16	370.7	1.626	24.72	0.102				
Lack-of-fit	10	11	335.1	1.626	33.51	0.148	4.70	3,431.64	0.051	0.000
Pure error	5	5	35.7	0.000	7.13	0.000				
Total	19	19								

X_1: Xylene concentration, X_2: Ethyl cyclopentane concentration, X_3: Methyl benzothiophene concentration

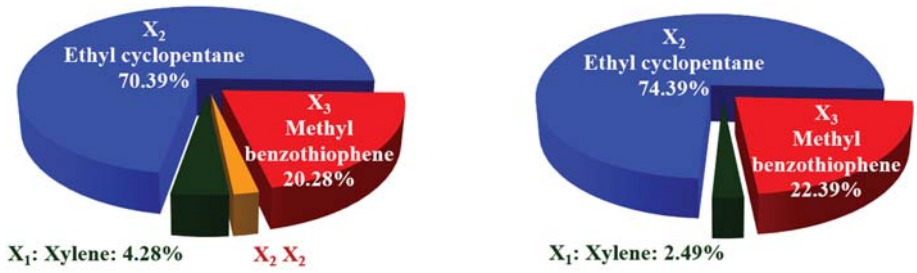

(a) Concentration of NIC in TDI **(b)** Density of PUF

Fig. 2. The order of magnitude and the impact of independent variables on response functions.

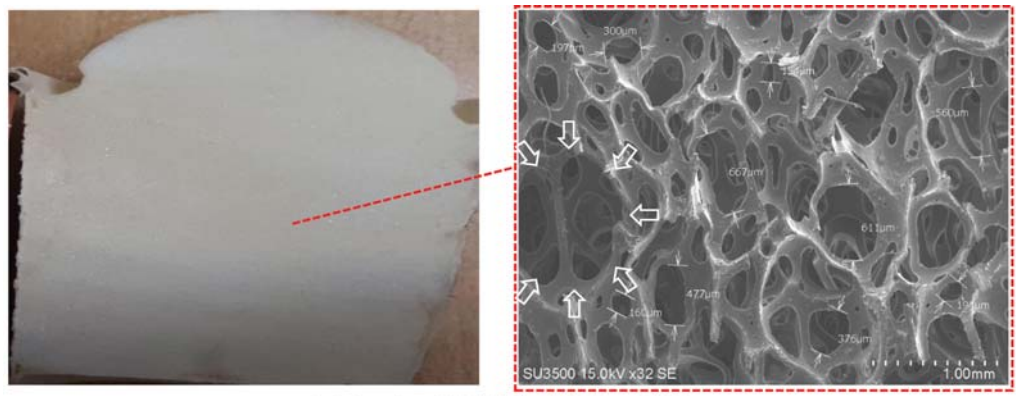

(a) density: 26.920 kg/m^3 (Run # 1)

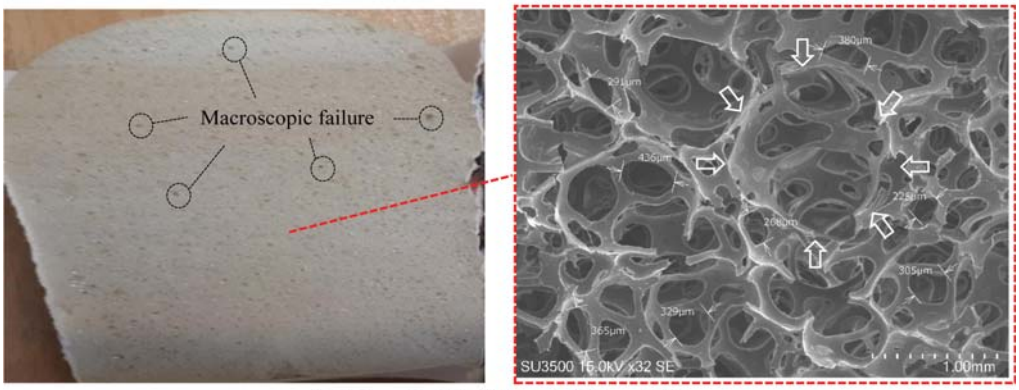

(b) density:33.490 kg/m^3 (Run # 3)

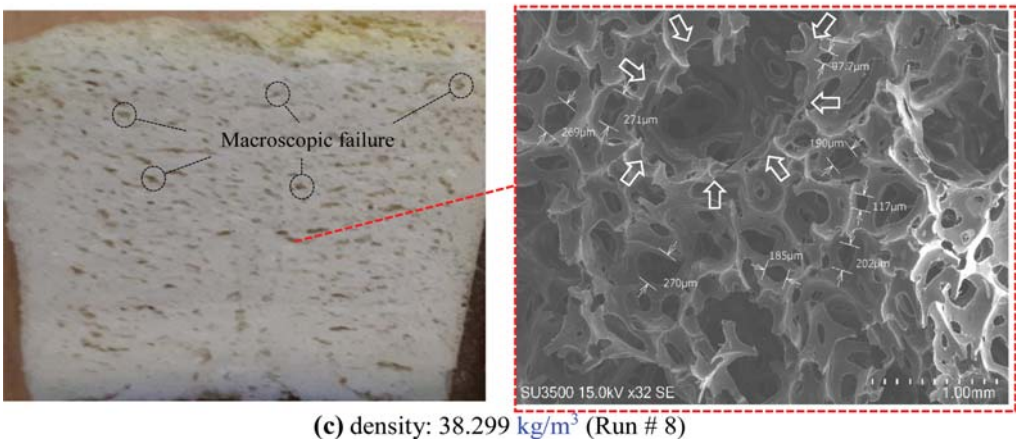

(c) density: 38.299 kg/m^3 (Run # 8)

Fig. 3. Macrographs and SEM micrographs of foams produced from toluene feed.

to study the effects of independent variables on response variables [23]. A three-factor experimental design with 20 runs was employed and the concentration of NIC in TDI (Y_1) and the density of PUF sample (Y_2) associated with predicted values was reported (Table 3). The experimental values of Y_1 and Y_2 varied in range of 19.2-109.4 mg/L and 26.920-38.299 kg/m^3, respectively, for all runs and the maximum number of porous sites within foam were produced at the lowest concentration of impurities (optimal conditions) and consequently the minimum density was achieved.

Statistical analysis using ANOVA (Table 4) revealed that single factors, i.e., ethyl cyclopentane, methyl benzothiophene, and xylene concentration with p-values of less than 0.0001 and quadratic term of Ethyl cyclopentane concentration with p-value of 0.01 were the most significant ones for concentration of NIC (Y_1). The ethyl cyclopentane, methyl benzothiophene, and xylene were also the most significant ones with p-values of less than 0.0001, whereas all quadratic terms and binary interactions were not significant for density (Y_2). The regression coefficient (R^2) values of the statistical data and predicted one were 96.76 and 92.30% for Y_1 and 99.17 and 98.14% for Y_2 which were in reasonable agreement with the adjusted R^2 (95.90% for Y_1 and 99.01% for Y_2). Moreover, the lack of fit value for the statistical data was insignificant, which suggested the accuracy of the data. To determine the adequacy of the data, further statistical analysis was carried out. The residuals have located very closed the normality line, approving the residuals to be normal (Figures not included).

The most significant factor affecting both the concentration of NIC in TDI and the density of PUF was the concentration of ethyl cyclopentane (representing non-aromatics class of impurities) by 70.39% and 74.39% contribution, respectively. Ethyl cyclopentane is thought to have been adsorbed by electrostatic forces on catalytic support, where its molecular structure and weight play a key role and cause further adsorption on the catalyst substrate. Unreacted DNT in the phosgenation reactor forms NIC as a result of the deactivation. The Pareto chart (Fig. 2) displays the order of factor importance for both responses as follows:

Ethyl cyclopentane>Methyl benzothiophene>Xylene

Regression equations for predicting the Y_1 and Y_2 were determined as follows according to the significant coded variables:

$$Y_1 \text{ (mg/L)}=54.23+5.51\,X_1+22.45\,X_2+12.04\,X_3+2.822\,X_2^2 \quad (11)$$

$$Y_2 \text{ (kg/m}^3\text{)}=32.588+0.541\,X_1+3.015\,X_2+1.654\,X_3 \quad (12)$$

Fig. 3 shows the macroscopic and SEM morphology of the PUF samples prepared in experimental runs 1, 3, and 8. The development of cracks and holes (seen by the naked eye) resulted in foam fracture and increased density as a consequence [24]. The size of the cells, cell size distribution, and structure thickness were comparable for all three foams examined. In addition to rigidity, the cellular structures of the polymer matrix influenced physical characteristics of foams [25,26]. Uniform well-defined cells with thinner walls associated with full-structural bonding for low-density PUF corresponding to the lower impurity concentration were observed (Fig. 3(a)). Increased impurities in Toluene led to increase in NIC content of TDI and density of PUF because of irregular shape and breakage in cells (Fig. 3(b)). The cells were much smaller, thicker in walls, and non-uniform/broken in shape for PUF sample of relatively highest density (Fig. 3(c)). The cell size ranged from 154 to 667 μm for the low-level, 225 to 436 μm for the middle-level, and 97.7 to 271 μm for the high-level of impurities concentration. The average PUF cell size decreased approximately 55% with the concentration of impurities increased by 114% for the investigated concentration range. This reduction in cell size had a notable effect on thermo-mechanical characteristics of rigid PUF [27].

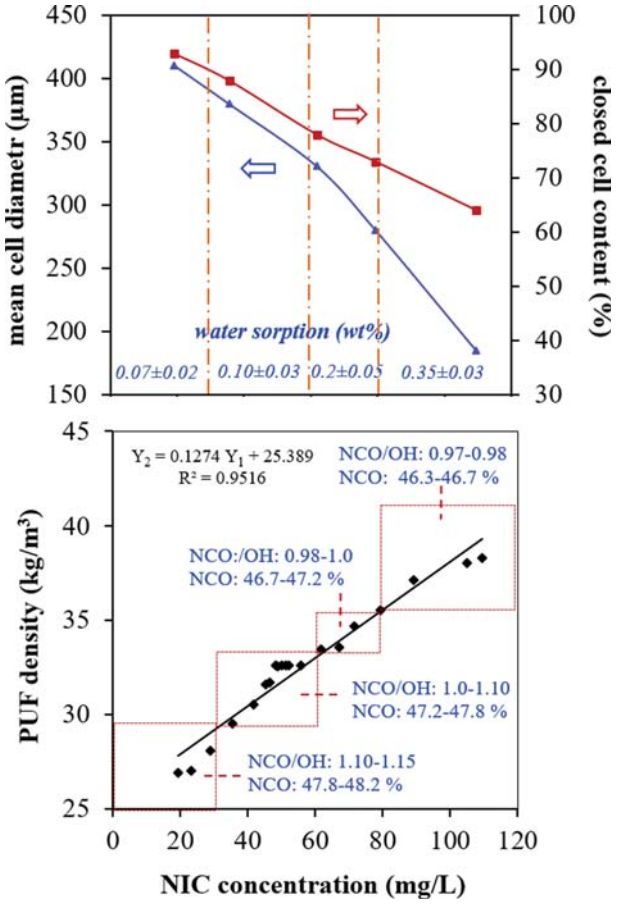

Fig. 4. Effect of TDI impurity on characteristics of PUF.

Fig. 4 demonstrates the relationship between NIC concentration in TDI (Y_1) and characteristics of synthesized PUFs. The measured densiy (Y_2) was almost laid down along the diagonal line, suggesting a linear relationship between both responses. The NCO content and NCO/OH mole ratio of samples decreased with concentration of NIC in TDI affecting the crosslink density and the rigidity of the PU network [28]. Higher content of NCOs results in a tightly crosslinked structure and leads to stronger bond strength. This strength of bonding also correlates with hydrogen bonding in the PU network. PUs are extensively hydrogen-bonded, with the proton donor coming from the -NH- group of the urethane linkage. The acceptor of hydrogen bonds may be in either in the hard segment (the carbonyl of the urethane group) or in the soft segment (an ester carbonyl or ester oxygen). Therefore, the extent of hydrogen bonding between C=O and N-H increased with the NCO/OH ratio.

Water sorption of the PUFs was also determined for some selected samples at 25 °C. It decreased with NCO content of sample. This can be attributed to water penetration during the short phase of curing PUF foams, which results in micro-void formation. An imperfect interfacial bonding between the two phases resulted in a higher degree of micro-voids, and consequently more water was absorbed.

The mean cell diameter was also calculated using "*ImageJ*" software from the SEM photographs. Owing to the rise in Toluene impurity and consequently the concentration of NIC in TDI, interfering with the cross-linking process of PUF, the number of non-full-structural bonding cells increased and subsequently increased the number of blind cells, resulting in a decrease in porosity and a rise in density associated with small cells.

The reaction between polyol and an excess amount of diisocyanate yielded a polyurethane prepolymer of NCO end-groups that further reacted with another polyol as a chain extender or crosslinking agent [29]. When the polyurethane was being developed, it organized into a chain link which was assembled by physical crosslinking (hydrogen bonding) between the hydrogen of the secondary amine group and the oxygen of carbonyl group. The density could be estimated from the lengths of proper polyurethane chains, where further crosslinking helped to form lower density. Linked networks of polymer struts and cell walls incorporated void spaces with captured air resulting in low density, high porosity/crushability, and strong potential for absorption capacity [24]. The NCO/OH ratio specifies the prepolymer's molecular weight and consequently the relative proportion of the urethane and urea groups in the final polymer chain. The final properties of polymer depend primarily on the chemical nature of the polymer building blocks, the NCO/OH ratio and the reaction sequence. NIC's low reactivity towards polyol also intensifies the reduction of the NCO content of impure TDI samples. The NCO groups' reactivity is enhanced by the presence of electron-with drawing groups. In general, increasing the TDI/polyol ratio during foaming process relieves the drawback of impurities. This approach does not, however, lead to high-quality foam and is not cost-effective either. The resulting short urethane chain was terminated with NCO when an excess quantity of TDI (more than stoichiometry) was used, and the hard segment formation suitable for proper chain extension could not be achieved.

Highest crosslinking took place when using the lowest concentration of impurities in TDI (Fig. 5). NIC impurities made a thermodynamic immiscibility and tension between the hard and soft segments and eventually contributed to separation of micro-phase. They interfered with the cross-linking process, broke and disordered the soft and hard segment chain during polymerization and led to crack weakens the structure's capacity as well as to increase polyurethane density that were undesirable issues. Moreover, the presence of OCN-R-NCO with two active side at the end led to a long polymer chain of highest crosslinking, whereas the presence of NIC (NO_2-R-NCO) with one active side at the end led to short polymer chain of lowest crosslinking [30].

In conclusion, Toluene impurities, as the source impurities, left a direct and indirect destructive effect on the PUF quality measured by density. Given the circumstances, it was extremely necessary in terms of quality and economics to maintain these impuri-

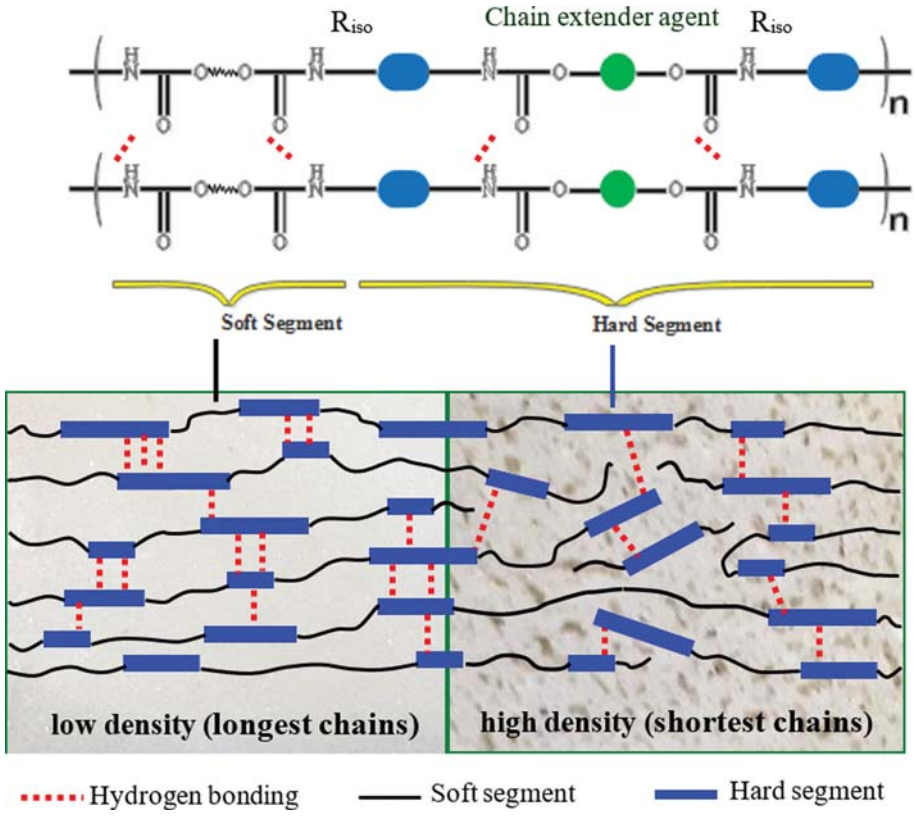

Fig. 5. Mechanistic effect of impure TDI on cross-linking process in PUF matrix.

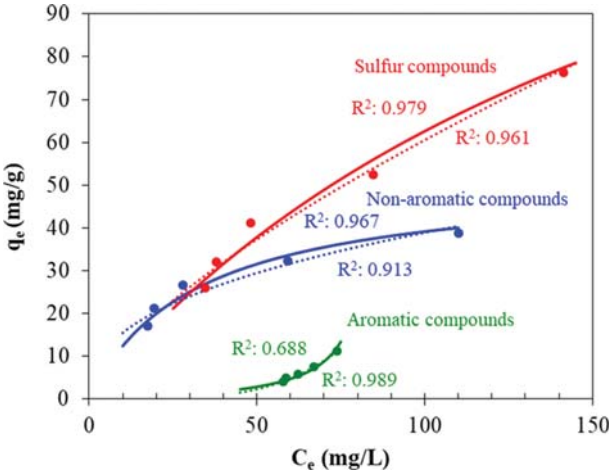

Fig. 6. Adsorption isotherms of aromatic, non-aromatic, and sulfur compounds on AC (dose: 1 to 5 g) at 20 °C (dash line: Freundlich, solid line: Langmuir).

ties at the lowest possible concentration. To accomplish this matter, the AC adsorption was suggested to be applied.

2. Adsorption Kinetics and Thermodynamics

AC is currently one of the most commonly used and promising adsorbents for the selective removal of sulfur compounds at relatively low temperature because of high surface area with weak polarity and uniform pore size distribution [31]. Some publications are available on the adsorption of organic molecules on AC from gas phase [32] and from aqueous phase [33]; however, studies on removal of these molecules from organic-liquid phase are quite limited [34]. AC is also considered to be the most common, effective, and practical solid adsorbent in this area.

The absorption experiments were applied to a selected industrial-grade toluene sample (Karoon Petrochemical Co.) with high impurities containing aromatics (96 mg·L^{-1}), non-aromatics (187 mg/L), and sulfur compounds (294 mg/L). Fig. 6 illustrates the adsorption capacity of AC for individual adsorbate during competitive adsorption from toluene at 20±1 °C and after 3 h. The final concentration of aromatic, non-aromatic, and sulfur compounds reached 58.1, 17.0, and 34.8 mg/L, respectively, after an adsorption cycle with 5 g AC.

Aromatics adsorption capacity was found to be lower than other compounds due to the similarity between the chemical structure of the toluene as the solvent and adsorbate molecules. In organic (aromatic) solvents, the affinity of aromatic hydrocarbons towards AC established a contest between solvent and adsorbate molecules and reduced the adsorption of both [32]. The molecular weight, concentration, dynamic diameter, and vapor pressure of adsorbate also affect the adsorption capacity of the adsorbent to a given pore diameter distribution. The adsorption of organic compounds on AC is principally physical depending on the electrostatic (van der Waals) force between them. Toluene and other aromatics can form π-π attraction between π-electrons of benzene rings and active sites of AC. The adsorption capacity increased with an increase in adsorbate molecular weight at equivalent concentrations of adsorbate. Moreover, if the pore diameter of adsorbent is far greater than the diameter of adsorbate, the pore functions as a channel and the adsorption capacity is low [35]. Therefore, a single ring aromatic compound of toluene or xylene cannot be adsorbed as much as large-molecules such as two-ring or possible polycyclic aromatic hydrocarbons formed during TDI synthesis [31]. It is noted that in impure toluene, a majority of one-ring aromatic compounds do not interfere with the adsorption of other compounds, including nonaromatic and sulfur compounds.

The non-aromatics sorption on AC is a complex phenomenon because of the non-aromatics molecular structure and the AC's energetically heterogeneous character. The active sites of various adsorptive powers might be spread over the solid surface. Hence, this process involves sophisticated interactions among the solvent, the adsorbent, and the adsorbate. Relatively high affinity of aromatic solvents for AC prevents other organics adsorption such as nonaromatic and sulfur compounds, and is entirely different from adsorption of organics from low affinity polar solvents for AC. Moreover, the dielectric constant slightly decreases from aromatic to nonaromatic hydrocarbons.

The adsorption capacity for sulfur compound was the highest among the organic impurities tested. It can be quickly adsorbed from liquid phase to the AC surface. A reduction in the number of aromatic rings in sulfur compounds induced a reduction in the quantity of adsorption because of a decrease in molecular weight and molecule size [34,35].

Table 5 summarizes the values of corresponding isotherm parameters. The R^2 values indicate that the Langmuir model (monolayer coverage) is in strong agreement with experimental data for non-

Table 5. Adsorption isotherms for removal of impurities from toluene

Model parameters	Simultaneous multicomponent adsorption (20 °C)			Single non-aromatic adsorption		
	Aromatics	Non-aromatics	Sulfur compounds	10 °C	20 °C	30 °C
Langmuir						
q_m	11,275	47.388	161.455	64.97	58.82	56.01
K_L	7.8×10^{-6}	0.038	0.006	0.010	0.015	0.031
R^2	0.688	0.967	0.979	0.982	0.982	0.975
Freundlich						
K_F	2.8×10^{-7}	6.133	2.436	6.346	3.598	2.233
1/n	4.061	0.401	0.698	0.417	0.491	0.577
R^2	0.989	0.913	0.961	0.998	0.962	0.965

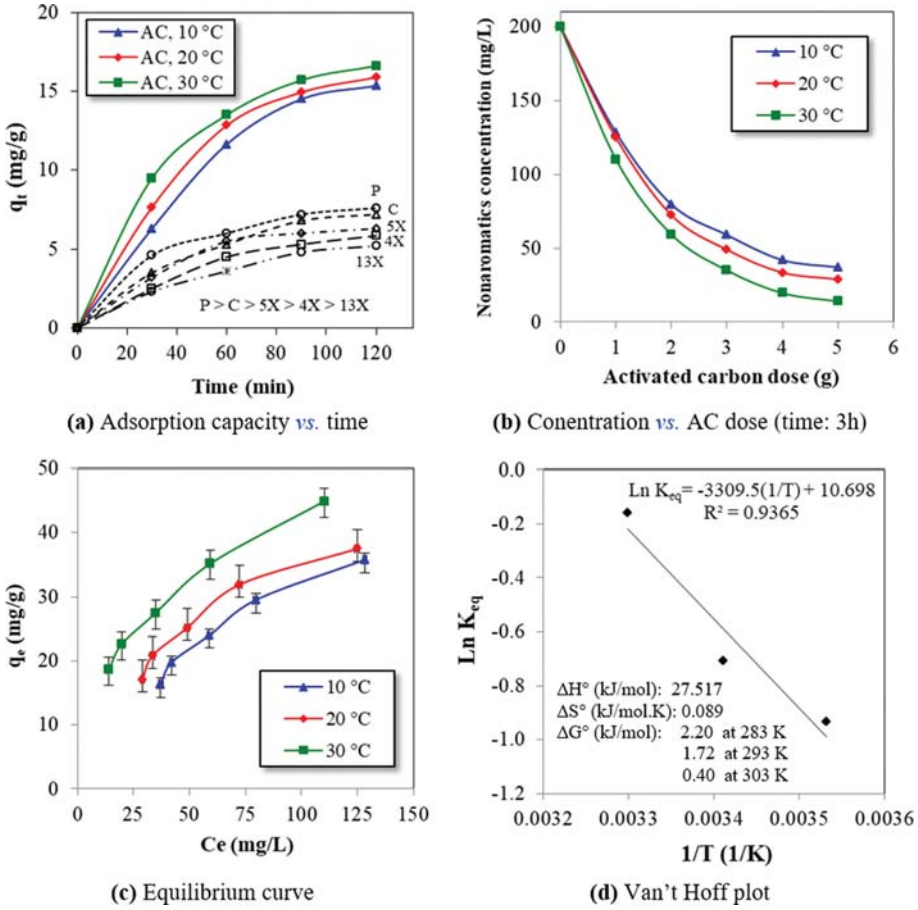

Fig. 7. Dynamics and thermodynamics of the non-aromatics adsorption (C_o: 200 mg/L, AC dose: 5 g).

aromatics and sulfur compounds while the Freundlich one is the best for aromatics.

Ethyl cyclopentane (representing non-aromatics compounds in real feedstock) impurity, as shown earlier, was the most influential factor and major impurity affecting PUF density. Given this fact, the adsorption efficiency of non-aromatics compounds was investigated on AC at an initial concentration of 200 mg/L (industrial grade) at various temperatures between 10 and 30 °C. A preliminary test was also conducted at mean temperature of 20 °C using different synthetic and natural zeolites, i.e., 13X, 4X, 5X, natural Clinoptilolite, and NaP-zeolite (Fig. 7) for comparison. The order of magnitude for zeolitic adsorption capacity was: NaP>Clinotilolite> 5X>4X>13X. The adsorption capacity of mineral zeolites for non-aromatics hydrocarbons was not more than haft of that for AC, suggesting AC's high potential for efficient organic impurity adsorption. As demonstrated in Fig. 7, the adsorption capacity of AC increased with temperature. The nature and thermodynamics of adsorption depend on the system under consideration, i.e., activation temperature and raw material used, which can be either exothermic or endothermic. Weak van der Waals forces are involved in physisorption, and it is beneficial at low temperatures or is exothermic [36]. Increasing the temperature decreases the viscosity of liquid and increases diffusion of adsorbate molecules within the pores of sorbent and also enhances the adsorption/desorption rate [37,38]. It is suggested that the co-adsorption of toluene and non-aromatic impurity occurs on the surface of AC, while rising temperature has resulted in more non-aromatic adsorption.

The values of ΔH^o, ΔS^o and ΔG^o were determined using the thermodynamic fitting curve (Fig. 7(d)). The positive-low value of heat of adsorption showed the endothermic nature of adsorption and weak binding forces between the adsorbed molecules and the AC surface. Positive-low value of Gibbs free energy changes suggested that the adsorption process was not spontaneous and thermodynamically unfavorable and it was mainly controlled by the physisorption. The positive ΔS^o of adsorption phenomenon indicated an increase in randomness at the solid-liquid interface.

The kinetic data (Fig. 7(a)) were fitted to both kinetic models, where there was a reasonable correlation between experimental data and models (Figures not included). According to the obtained-high correlation coefficient (R^2: 0.999), this confirmed that the adsorption kinetic follows a first-order model with k_1 (min): 0.0248, while the rate constant for first-order kinetic model k_2 (g/mg·min) is 0.00115 (R^2: 0.998). The much closed regression coefficients for both models indicated that the first-order kinetic may also be applied, since this case is not concerned with the adsorption of a pure-single component.

Batch mode adsorption using AC led to toluene with an appropriate concentration of impurities for TDI synthesis. The proposed

adsorption method for purifying industrial grade Toluene feed can be applied practically on a large-scale and in continuous mode to achieve a very low concentration of impurities. More work is required to study the adsorption dynamics for scale-up purposes.

CONCLUSIONS

The undesirable effect of three organic impurities in model toluene, namely xylene, ethyl cyclopentane, and methyl benzothiophene, was investigated on pilot-scale synthesis of toluene diisocyanate and rigid polyurethane foam (PUF). They represent aromatic, non-aromatic and sulfur impurities class of organic impurities in industrial-grade toluene, respectively. Activated carbon was successfully applied for simultaneous adsorption of mentioned organic impurities and the following points were extracted from this study:

- The size of the cells, cell-size distribution, and cell wall thickness were affected and quantified by different doses of impurities. As expected, lower impurities resulted in a more closed-cell structure with uniform cell sizes.
- Among the impurities studied, ethyl cyclopentane (non-aromatics class) and xylene (aromatic class) had the most and least impact on foam density, respectively. A similar result was observed for concentration of 2-Nitro-4-isocyanatotoluene in synthesized toluene diisocyanate.
- Competitive adsorption of a real feed involving aromatic, non-aromatic and sulfur classes of impurities showed that the order of magnitude for maximum adsorption capacity was sulfur compounds>non-aromatics>aromatics. Adsorption capacity increased with molecular weight and size of molecule such that larger molecules (non-aromatics and sulfur compounds) adsorbed more than single ring aromatic molecules (toluene and xylene).
- The isotherm models for adsorption on activated carbon indicated that the aromatics obey Freundlich isotherm and the non-aromatics and sulfur compounds adopt Langmuir isotherm.

ACKNOWLEDGEMENT

The authors gratefully acknowledge Mr. Abbas Akbari (ORCID iD: https://orcid.org/0000-0002-1092-1108) of the Chemical Engineering Department of Razi University (Iran) and the R&D Center of Karoon Petrochemical Company (Iran) for the great support to perform this study.

NOMENCLUATURE

AC : activated carbon
CCD : central composite design
C_e : equilibrium concentration of impurities [mg/L]
C_o : initial concentration of impurities [mg/L]
DAT : 2,4-Diaminotoluene
DNT : 2,4-Dinitrotoluene
k_i : constant of adsorption rate [1/min]
k_2 : constant of adsorption rate [g/mg·min]
K_{eq} : equilibrium constant (q_e/C_e)
K_F : Freundlich constant [L^n $mg^{1/n}$/g]
K_L : net enthalpy of the adsorption [L/mg]
m : mass of adsorbent [g]
n : Freundlich constant
NIC : 2-Nitro-4-isocyanatotoluene
PUF : polyurethane foam
q_e : equilibrium adsorption capacity [mg/g]
q_m : maximum adsorption capacity [mg/g]
q_t : amount of impurities adsorbed at any time [mg/g]
R : ideal gas constant [kJ/mol·K]
RSM : response surface methodology
SEM : scanning electron microscopy
t : time [min]
T : temperature [K]
TDI : toluene diisocyanate
V : volume of solution [L]
X_1 : concentration of Xylene [mg/L]
X_2 : concentration of Ethyl cyclopentane [mg/L]
X_3 : concentration of Methyl benzothiophene [mg/L]
Y_1 : concentration of NIC in TDI [mg/L]
Y_2 : density of each PUF sample [kg/m^3]
ΔH^o : standard enthalpy change [kJ/mol]
ΔG^o : standard Gibbs free energy change [kJ/mol]
ΔS^o : standard entropy change [kJ/mol·K]

REFERENCES

1. H. Singh, T. P. Sharma and A. K. Jain, *J. Appl. Polym. Sci.*, **106**, 1014 (2007).
2. P. Cinelli, I. Anguillesi and A. Lazzeri, *Eur. Polym. J.*, **49**, 1174 (2013).
3. G. Zhang, Q. Zhang, Y. Wu, H. Zhang, J. Cao and D. Han, *J. Appl. Polym. Sci.*, **134**, 45582 (2017).
4. P. Mondal and D. V. Khakhar, *J. Appl. Polym. Sci.*, **93**, 2830 (2004).
5. S. H. Kim, B. K. Kim and H. Lim, *Macromol Res.*, **16**, 467 (2008).
6. P. Ferkl, I. Kršková and J. Kosek, *Chem. Eng. Sci.*, **176**, 50 (2018).
7. N. V. Gama, A. Ferreira and A. Barros-Timmons, *Materials*, **11**, 1841 (2018).
8. K. Ashida, *Polyurethane and related foams: chemistry and technology*, CRC Press, Taylor & Francis Group, Boca Raton, Florida, USA (2006).
9. H. Lim, S. H. Kim and B. K. Kim, *Polym. Adv. Technol.*, **19**, 1729 (2008).
10. M. Zuber, K. M. Zia, M. A. Iqbal, Z. T. Cheema, M. Ishaq and T. Jamil, *Korean J. Chem. Eng.*, **32**, 184 (2015).
11. I. Javni, W. Zhang and Z. S. Petrović, *J. Appl. Polym. Sci.*, **88**, 2912 (2003).
12. L. Shufen, J. Zhi, Y. Kaijun, Y. Shuqin and W. K. Chow, *Polymer Plast. Technol. Eng.*, **45**, 95 (2006).
13. M. Fiayyaz, K. M. Zia, M. Zuber, T. Jamil, M. K. Khosa and M. A. Jamal, *Korean J. Chem. Eng.*, **31**, 644 (2014).
14. D. C. Allport, D. C. Gilbert and S. M. Outterside, *MDI and TDI: safety, health and the environment: a source book and practical guide*, John Wiley & Sons Ltd., Chichester, West Sussex, England (2003).
15. M. Thirumal, D. Khastgir, N. K. Singha, B. S. Manjunath and Y. P. Naik, *J. Appl. Polym. Sci.*, **108**, 1810 (2008).
16. A. Belkadi and D. Edouard, *Chem. Eng. Process: Process Intensif.*, **86**, 64 (2014).

17. W. J. Seo, H. C. Jung, J. C. Hyun, W. N. Kim, Y. B. Lee, K. H. Choe and S. B. Kim, *J. Appl. Polym. Sci.*, **90**, 12 (2003).
18. C. H. Lee, K. J. Kim and S. K. Ryu, *J. Chem. Eng. Jpn.*, **25**, 585 (1992).
19. Y. Hou, L. Xu, Z. Wei, Y. Liu, X. Li and S. Deng, *J. Taiwan Inst. Chem. Eng.*, **45**, 1428 (2014).
20. HG/T 2409, Determination of isocyanate group content in polyurethane performed polymer (1992).
21. ASTM D1622-08, Standard Test Method for Apparent Density of Rigid Cellular Plastics (2008).
22. ASTM D2850-15, Standard Test Method for Unconsolidated-undrained Triaxial Compression Test on Cohesive Soils (2007).
23. J. Behin, A. Akbari, M. Mahmoudi and M. Khajeh, *Water. Res.*, **121**, 120 (2017).
24. L. Marsavina, D. M. Constantinescu, E. Linul, T. Voiconi and D. A. Apostol, *Eng. Failure Anal.*, **58**, 465 (2015).
25. G. Sung, H. Choe, Y. Choi and J. H. Kim, *Korean J. Chem. Eng.*, **35**, 1045 (2018).
26. A. Noreen, K. M. Zia, M. Zuber, S.Tabasum and M. J. Saif, *Korean J. Chem. Eng.*, **33**, 388 (2016).
27. M. Thirumal, D. Khastgir, N. K. Singha, B. S. Manjunath and Y. P. Naik, *J. Appl. Polym. Sci.*, **108**, 1810 (2008).
28. G. Sung and J. H. Kim, *Korean J. Chem. Eng.*, **34**, 1222 (2016).
29. A. Cornille, R. Auvergne, O. Figovsky, B. Boutevin and S. Caillol, *Eur. Polym. J.*, **87**, 535 (2017).
30. S. Huo, G. Wu, J. Chen, G. Liu and Z. Kong, *Korean J. Chem. Eng.*, **33**, 1088 (2016).
31. K. Sakanishi, H. Farag, S. Sato, A. Matsumura and I. Saito, *Am. Chem. Soc. Div. Fuel Chem.*, **48**, 524 (2003).
32. M. A. Lillo-Ródenas, D. Cazorla-Amorós and A. Linares-Solano, *Carbon*, **43**, 1758 (2005).
33. C. Moreno-Castilla, *Carbon*, **42**, 83 (2004).
34. A. M. Dowaidar, M. S. El-Shahawi and I. Ashour, *Sep. Sci. Technol.*, **42**, 3609 (2007).
35. L. Li, Z. Sun, H. Li and T. C. Keener, *J. Air Waste Manag. Assoc.*, **62**, 1196 (2012).
36. S. V. Patil, L. G. Sorokhaibam, V. M. Bhandari, D. J. Killedar and V. V. Ranade, *J. Environ. Chem. Eng.*, **2**, 1495 (2014).
37. M. Fayazi, M. A. Taher, D. Afzali and A. Mostafavi, *Anal. Bioanal. Chem. Res.*, **2**, 73 (2015).
38. L. Fei, J. Rui, R. Wang, Y. Lu and X. Yang, *RSC Adv.*, **7**, 23011 (2017).